Setting the Clock for Fail-Safe Early Embryogenesis

Rolf Fickentscher, Philipp Struntz, and Matthias Weiss

Phys. Rev. Lett. **117**, 188101 — Published 24 October 2016

DOI: 10.1103/PhysRevLett.117.188101

Setting the clock for fail-safe early embryogenesis

Rolf Fickentscher, Philipp Struntz, and Matthias Weiss
Experimental Physics I, University of Bayreuth, Universitätsstr. 30, D-95440 Bayreuth, Germany

Embryogenesis of the small nematode *Caenorhabditis elegans* is a remarkably robust self-organization phenomenon. Cell migration trajectories in the early embryo, for example, are well explained by mechanical cues that push cells into positions where they experience least repulsive forces. Yet, how this mechanically guided progress in development is properly timed has remained elusive so far. Here we show that cell volumes and division times are strongly anti-correlated during early embryogenesis of *C. elegans* with significant differences between somatic cells and precursors of the germline. Our experimental findings are explained by a simple model which in conjunction with mechanical guidance can account for fail-safe early embryogenesis of *C. elegans*.

PACS numbers: 05.65.+b, 87.18.-h, 87.64.M-, 87.18.Hf, 87.17.Aa

The small transparent nematode *Caenorhabditis elegans* is a simple and well-studied organism whose natural habitat is the soil. Being exposed to fluctuating environmental conditions, *C. elegans* has developed robust strategies to ensure successful reproduction cycles: A chitin-based ellipsoidal egg shell protects the worm's progeny from external threats, from the zygote until hatching of the worm. Moreover, *C. elegans* undergoes an invariant cell division scheme during embryogenesis [1], i.e. all adult worms have the same number of cells ('eutely'). Eutely requires the autonomously progressing developmental program inside the egg shell to be robust and fail-safe already during early embryogenesis: Important founder cells emerge in this stage, and they need to migrate towards biologically meaningful spatial positions to support body axis formation and organ development [1], e.g. via neighborhood-sensitive signaling pathways.

C. elegans not only undergoes an invariant cell division scheme but also cell migration paths in the early embryo are almost invariant between different individuals [2]. These invariant cell migration paths have been explained consistently with a simple and robust mechanical model in which cells interact via repulsive potentials within the confining egg shell [2]. Based on experimental input data like cell division times and axes, the model accurately predicted cells to relax towards positions of least repulsion after mitosis, e.g. into a non-trivial planar configuration in the 4-cell stage. These observations indicate that part of the robustness of the early developmental program of *C. elegans* is based on basic physical cues and forces rather than on elaborate biochemical signaling pathways.

However, relying on experimental input data, the model did not allow any insights as to how internal decisions of individual cells, e.g. on their cell cycle duration, are integrated to achieve those force fields that push all cells into their physiological positions. Phrasing it provocatively: How do individual cells know that dividing right now is a good choice for a meaningful and robust mechanically driven arrangement of all cells in the embryo?

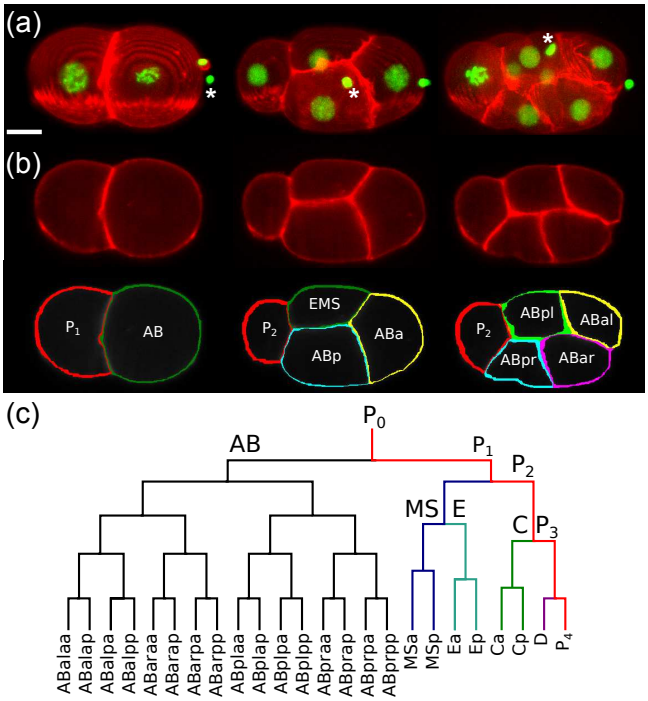

FIG. 1: (a) Maximum intensity projection of image stacks taken with SPIM on *C. elegans* embryos of strain OD95 in which fluorescent markers stain the plasma membrane (red) and chromatin (green). White asterisks indicate nuclear bodies that are known to be irrelevant for embryogenesis. Scale bar: 10 μm. (b) Corresponding individual xy-slices of the red channel (upper panel) and results of the membrane segmentation with cell names assigned (lower panel). (c) Early invariant cell lineage tree of *C. elegans* with cells of the AB, P, MS, and C lineages being highlighted in black, red, blue, and green, respectively.

To address this question, we have monitored the development of *C. elegans* embryos until the onset of gastrulation (starting beyond the 24-cell state) with single plane illumination microscopy (SPIM) [2–6]. Using an updated version of our previously described SPIM setup [2, 7] that allows for longterm three-dimensional

dual-color imaging, we monitored eggs from *C. elegans* strains (i) XA3501, (ii) OD95, and (iii) OD58 in which the plasma membrane and chromatin are stained by fluorescent proteins [8]. Representative images of strain OD95 are shown in Fig. 1a,b. For each image stack a full three-dimensional reconstruction was done to determine cell volumes and shapes (see Fig. 1b for representative segmentation results). Segmented images and tracking of nuclei [2] allowed us to identify cells according to the nematode's invariant lineage tree (Fig. 1c).

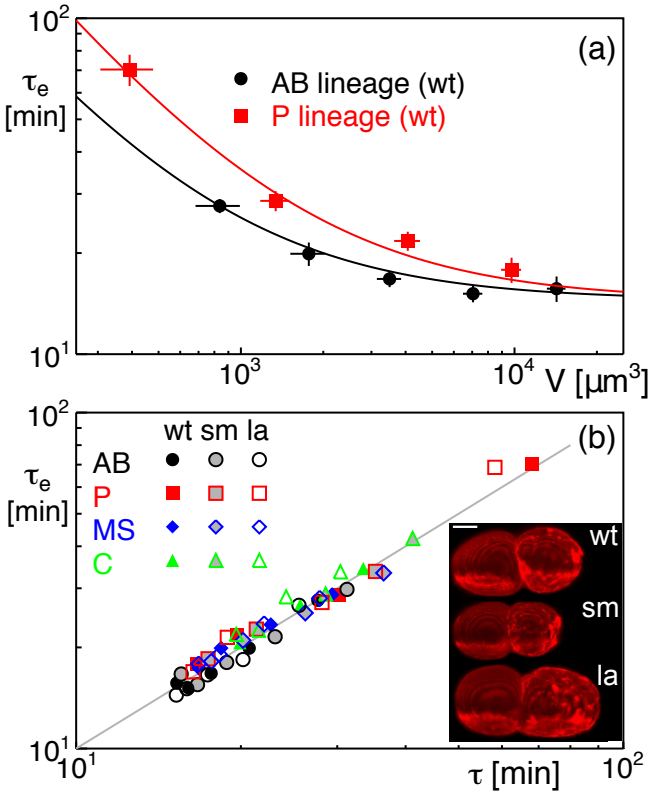

FIG. 2: (a) Experimentally determined cell lifetimes τ_e are clearly anti-correlated with the cell's volume V, e.g. in the AB lineage (black circles) and in the P lineage (red squares). Data were taken with untreated embryos (wt) at 22.5°C and averaged over each generation of cells. Error bars indicate standard deviations between different embryos ($n = 8$). Data are well described by Eq. (1) (full lines). (b) Cell cycle times τ obtained via Eq. (1) show an excellent agreement with experimentally determined cell division times, τ_e for lineages AB, P, MS, and C in untreated (wt) and RNAi-treated embyros with smaller (sm) and larger (la) size of the zygote P_0 (cf. inset in the lower right corner). Data were taken at 22.5°C. Values for τ were obtained from Eq. (1) with $\tau_M = 870$s and slight variations of α to account for lineage-specific behavior ($\alpha = 0.66$, 1.26, 0.72, $0.84 \times 10^6 \mu\text{m}^3\text{s}$, for AB, P, MS, and C lineage, respectively, irrespective of any RNAi treatment).

Searching for signatures of how decisions of individual cells are coupled to the mechanics of the rest of the embryo, we observed that cell volumes, V, and cell lifetimes, τ_e, are anti-correlated during early embryogenesis (in particular beyond the 12-cell state, i.e for $V \lesssim 3000\mu\text{m}^3$; see Fig. 2a for two examples). Here, the cell lifetime τ_e is defined as the period from the cell's emergence up to its division into two daughter cells (period from anaphase $n-1$ to anaphase n). In agreement with previous observations [9] the actual mitosis period (M phase) was approximately constant for all cells, whereas the preceding preparation period (S phase) varied markedly with cell size. Since cells cycle only between S and M phase during early embryogenesis, cellular lifetimes are determined by these two periods, i.e. $\tau_e = \tau_S(V) + \tau_M$. Empirically, we found that keeping τ_M constant and setting $\tau_S(V) \sim 1/V$ provided very good heuristic fits to our experimental data (see representative examples in Fig. 2a).

The empirically found variation $\tau_S \sim 1/V$ can be rationalized by considering a limiting component that determines the transition rate from S to M phase. This could be, for example, the number of nuclear pore complexes (NPCs) which we use here as a representative to develop our argument. NPCs mediate the translocation of M-phase promoting factors (MPFs), e.g. activated Cdk1 [10], into the nucleus. Since binding to and translocation through NPCs is a slow process that requires an elaborate set of support proteins, e.g. importins, the growth of the MPFs' nuclear concentration can be written as $da/dt = N\gamma c$. Here, N is the number of NPCs in the cell and γ is the typical translocation rate per NPC; a and c denote the MPFs' nuclear and cytoplasmic concentration, respectively. Simplifying the transition to M phase as an integrate-and-fire process, mitosis will start upon reaching a critical nuclear concentration, a^*. The time needed to reach this threshold is hence $\tau_S = 1/(N\gamma)$.

Since early embryogenesis is blastomeric, i.e. a volume-conserving process, with little to no transcription [11], the total number of the limiting component, N_0, is assumed to be constant (see below for a discussion). During mitosis, the nuclear envelope of the mother cell is disassembled and NPCs are partitioned into the emerging daughter cells, i.e. the number of NPCs in each cell can be approximated as $N = N_0 V/v_0$. In the most straightforward scenario, v_0 is simply the embryo's invariant total volume, yet also deviations due to biochemically asymmetric divisions are possible (see discussion below). The time needed for a complete cell cycle therefore is given by

$$\tau = \frac{\alpha}{V} + \tau_M \quad \text{with} \quad \alpha = \frac{v_0}{N_0\gamma} \,. \tag{1}$$

Indeed, Eq. (1) yields an excellent prediction of experimentally observed cell lifetimes, i.e. $\tau_e \approx \tau$, not only for the AB and P lineages but also for MS and C lineages (Fig. 2b). Here, $\tau_M = 870$s was held constant and only minor variations of α were needed for AB, MS, and C lineages ($\alpha = 0.66$, 0.72, $0.84 \times 10^6 \mu\text{m}^3\text{s}$) whereas the P lineage required an approximately twofold larger value

($\alpha = 1.26 \times 10^6 \mu m^3 s$). We attribute this significantly higher value of α mainly to the distinct biochemical composition of the P lineage. Being precursors of the adult worm's germline, fluid droplets of RNA and proteins [12], the so-called P-granules, are deposited in cells of the P lineage due to geometrically and biochemically asymmetric cell divisions [1]. P-granules have been implicated to sequester constituents of the NPCs [11, 13], hence reducing γ and/or increasing the effective reference volume v_0 in Eq. (1). The P lineage therefore can be expected to show a markedly higher value for α than other lineages.

In addition, lineage-specific differences in the parameter α may also be linked to a temporal increase of the limiting component: Updating the derivation of Eq. (1) to allow for an increase of the limiting component, $N(t) = N_0(1+\beta t)$, resulted in decreasing values of α for increasing production rates β while the gross scaling of Eq. (1) remained unaffected [8]. Since the transcription rate beyond the 4-cell stage is enhanced in somatic cells [11], germline precursors can therefore be expected to display values $\alpha_P > \alpha_{AB}$.

We would like to emphasize again that Eq. (1) may also be derived using limiting components other than NPCs. It is worth noting, however, that a reduction of functional NPCs via RNAi indeed resulted in delayed mitosis [14], in agreement with our above reasoning.

We next tested whether the favorable agreement of Eq. (1) and experimental data is a robust one. First, we treated adult worms with RNAi constructs against ima3 and C27D9.1 [15] which led to significantly smaller and larger embryos, respectively (cf. Fig. 2b, inset). Since changes in the zygote's overall volume should affect N_0 and v_0 equally, values for α should remain constant, i.e. experimentally determined lifetimes τ_e of RNAi-treated embryos were expected to follow τ from Eq. (1) with the same parameters used for untreated embryos (cf. previous paragraph). Indeed, our experimental data confirmed this prediction, i.e. lineages AB, P, MS, and C of the RNAi-treated embryos did not require any adjustment of parameters (Fig. 2b).

As a second test for the robustness of Eq. (1), we asked whether the observed anti-correlation of cell volumes and lifetimes holds within the animal's natural physiological temperature range (about 15-25°C). Data presented so far were acquired at 22.5°C. Since biochemical reactions in the embryo govern the timing of cell divisions, we expected cell doubling times to show an Arrhenius scaling, $\tau_D \sim \exp(T_0/T)$. We reasoned that parameters in Eq. (1) should show the same scaling if our theory is applicable within the animal's physiological temperature range. In line with our expectations and previous reports [16], we observed that experimentally determined cell doubling times followed an Arrhenius scaling with $T_0 \approx 7417K$ (Fig. 3a). The same scaling was seen for parameter α in Eq. (1) for all lineages while τ_M showed a somewhat weaker temperature dependence (Fig. 3a). Small deviations from an Arrhenius scaling around 25°C most likely are due to the previously reported thermal limit of proper embryogenesis [16]. Hence, our quantitative description of a size-dependent cell lifetime in early embryogenesis is valid within the development-permissive temperature range of the animal.

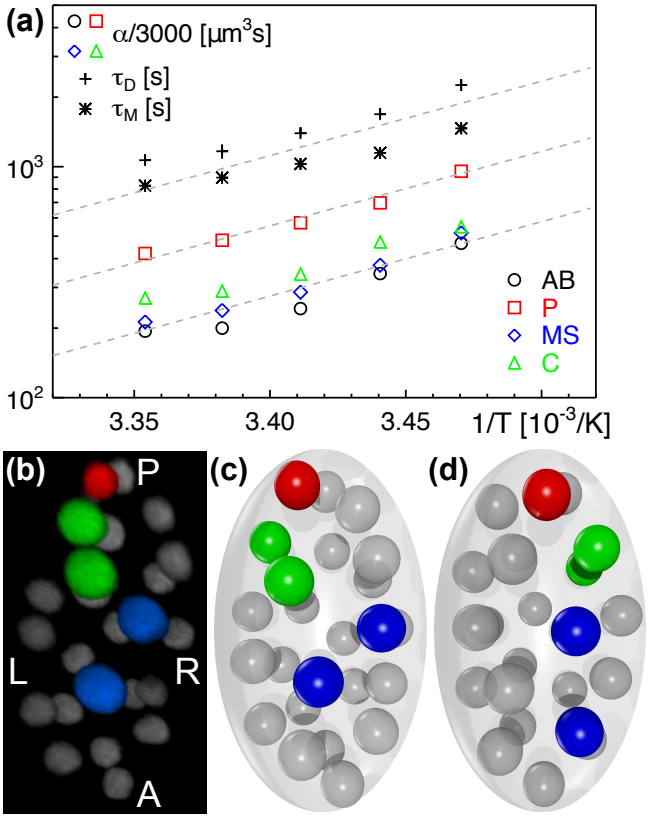

FIG. 3: (a) Experimentally determined cell doubling times τ_D (crosses) follow an Arrhenius scaling $\sim \exp(7417K/T)$ (dashed grey lines). Parameter α [Eq. (1)] follows the same scaling (open symbols) irrespective of the lineage, whereas τ_M (asterisks) shows a slightly less strong temperature dependence. Deviations from the Arrhenius scaling around 25°C reflect the thermal limit of the worm's development [16]. (b) Projection of SPIM images perpendicular to the dorsal-ventral body axis taken on an embryo in the 24-cell stage (strain OD95). Nuclei of cells P_4 (red), Ea/Ep (green), and MSa/MSp (blue) are highlighted; A/P, and L/R indicate anterior, posterior, left, and right faces of the embryo. (c) The experimentally observed phenotype is faithfully reproduced by model simulations that consider Eq. (1) and cell-cell repulsion within the confining egg shell. (d) Aberrant phenotypes are observed when cell divisions of the P lineage are enforced to follow Eq. (1) with parameters of the AB lineage.

Next, we explored if and to which extent the robust coupling of cell cycle durations and volumes can help to integrate decisions of individual cells to facilitate proper development of the entire embryo. To this end, we revisited the previously mentioned model approach for mechanical determination of embryonic cell migration [2]. In

brief, cell motion is described by Langevin equations with repulsive forces arising from cell-cell and cell-eggshell interactions. Lacking a description for cell-internal (biochemical) decisions, cell divisions are treated as instantaneous events, i.e. dividing cells are replaced by two daughter cells between two iteration steps. In previous work [2], we had fixed all division times via experimental input data. As a result, simulated cellular arrangements were seen to agree with experimental data up to the 12-cell state even when cell division times were detuned. Going beyond this approach, we have replaced now the input of cell division times by predictions of Eq. (1) using cell volumes (see supplemental text and Fig. S3, [8]). In addition to replacing a large set of experimental input parameters, our refined SPIM setup also allowed us to compare now experimental observations and simulations up to the 24-cell state.

Using the above determined set of parameters, α and τ_M, we were indeed able to reproduce cellular arrangements and migration trajectories of developing embryos up to the 24-cell stage (Fig. 3b,c). A temporally resolved correlation of data from experiment and simulation is shown in Fig. S1 [8]. Beyond the 24-cell stage gastrulation with an active inwards-directed motion of cells sets in which is not included in the model. Typical positional deviations between our simulations and the respective experimental SPIM data are in the range of experimental uncertainties ($\sim 4\mu$m, cf. [2]) with $> 99\%$ of 300 simulation runs leading to the correct phenotype. Hence, cell positions in the early embryo predicted by the mechanical model and Eq. (1) compare favorably to experimental data.

Based on the very good agreement between model and experimental data, we sought to determine via simulations which are the crucial ingredients for proper embryogenesis. As a first step we examined the influence of relative cell volumes by enforcing all cell divisions to be (geometrically) symmetrical, i.e. asymmetric divisions in the P lineage were suppressed. This artificial constraint leads to enlarged cells of the P, E, MS, and C lineages on expense of the AB lineage and hence to altered cell division timing [Eq. (1)]. As a result, deviations of cell positions in model and experiment increased slightly, yet the correct phenotype (i.e. the correct cell arrangement in the 24-cell state) was maintained in $> 99\%$ of 300 simulation runs.

In a second step, we altered only the timing of cell division. As stated above, the parameter α in Eq. (1) is different between the P lineage and all other, somatic cell lineages. We therefore enforced in the model that all cell divisions of the P lineage follow the scaling of somatic cells, i.e. $\alpha_P = \alpha_{AB}$, while keeping cell division asymmetries intact. This constraint lead to significant changes: About 10% of 300 simulation runs assumed now a drastically altered phenotype (Fig. 3d) that deviated strongly from the unperturbed embryo (Fig. 3b,c). Cells Ea and Ep, for example, are shifted to the right-hand side of the embryo instead of being situated on the left ventral segment. Since Ea and Ep are the first cells that drive gastrulation, a wrong positioning of them has a severe impact on subsequent steps of the embryogenesis. Given that a change in α of the P lineage should also be accompanied by a loss of asymmetric cell divisions, we also added the constraint of purely symmetric cell divisions to the condition $\alpha_P = \alpha_{AB}$ in subsequent simulations. In this case, even 25% of 300 simulation runs resulted in aberrant phenotypes like the one shown in Fig. 3d. In fact, in this scenario a 3:1 bifurcation of phenotypes is seen beyond the 12-cell stage (supplement, Fig. S1) whereas a robust arrangements is seen before, in agreement with our previous work [2]. Hence, cell division timing becomes increasingly important for proper embryogenesis as the number of cells increases.

The reason for the occurence of these aberrant phenotypes is rooted in a too quick succession of cell divisions which prevents cells from relaxing into their stable positions. In fact, daughter cells of EMS (i.e. MS and E) are situated in somewhat instable, stressed positions directly after the division of EMS along the anterior-posterior axes *in vivo*. This instable situation is relaxed by a drift of MS to the right ventral side of the embryo in conjunction with a shift of its sister cell E to the left ventral side. Altering α_P to the value of the somatic lineages speeds up cell division of P_2 to occur too fast after EMS' division. As a consequence, cells MS and E find themselves in an even more stressed position which is relaxed in a significant fraction of embryos via an aberrant movement of E. Embryogenic failures therefore emerge via slightly wrong cell positions in the 8-cell state that are caused by a premature division of P_2. With cells becoming smaller in each division cycle this small perturbation can grow, eventually leading to severe, detectable defects beyond the 12-cell stage (supplement, Fig. S1). Coupling of cell volumes and division timing, in particular a significantly larger value of α_P, therefore renders cellular arrangements more deterministic and robust.

Our results show how combining mechanical forces with a coupling of cell volumes and cycle times ensures a robust cellular arrangement in *C. elegans* embryos, hence supporting a fail-safe embryogenesis. Asymmetric cell divisions are crucial in this context as they fine-tune the local volume occupancy concomitant to significantly slowing down the cell cycle timing in precursors of the germline. As a consequence, sufficient time is available for the mechanically driven migration of cells to their native positions before subsequent cell divisions alter the force fields.

Financial support from DFG grant WE4335/3-1 and GIF grant I-1211-309.13/2012 are gratefully acknowledged. Worm strains were provided by the CGC, which is funded by NIH Office of Research Infrastructure Programs (P40 OD010440).

[1] *Wormbook*, URL `http://www.wormbook.org`.

[2] R. Fickentscher, P. Struntz, and M. Weiss, Biophys J **105**, 1805 (2013).

[3] P. J. Keller, A. D. Schmidt, J. Wittbrodt, and E. H. Stelzer, Science **322**, 1065 (2008).

[4] J. Huisken, J. Swoger, F. Del Bene, J. Wittbrodt, and E. H. K. Stelzer, Science **305**, 1007 (2004).

[5] J. Huisken and D. Y. R. Stainier, Development **136**, 1963 (2009).

[6] Y. Wu, A. Ghitani, R. Christensen, A. Santella, Z. Du, G. Rondeau, Z. Bao, D. Colon-Ramos, and H. Shroff, Proc Natl Acad Sci U S A **108**, 17708 (2011).

[7] P. Struntz and M. Weiss, J. Phys. D **49**, 044002 (2016).

[8] For details see Supplemental Material [url], which includes Refs. [11, 17, 18].

[9] C. A., A. Desai, and K. Oegema, Cell **137**, 926 (2009).

[10] Q. Yang and J. Ferrell, Nat Cell Biol **15**, 519 (2013).

[11] E. Voronina and G. Seydoux, Development **137**, 1441 (2010).

[12] A. A. Hyman, C. A. Weber, and F. Julicher, Annu Rev Cell Dev Biol **30**, 39 (2014).

[13] D. L. Updike, S. J. Hachey, J. Kreher, and S. Strome, J Cell Biol **192**, 939 (2011).

[14] D. Joseph-Strauss, M. Gorjanacz, R. Santarella-Mellwig, E. Voronina, A. Audhya, and O. Cohen-Fix, Dev Biol **365**, 445 (2012).

[15] B. Sonnichsen, L. B. Koski, A. Walsh, P. Marschall, B. Neumann, M. Brehm, A. M. Alleaume, J. Artelt, P. Bettencourt, E. Cassin, et al., Nature **434**, 462 (2005).

[16] M. L. Begasse, M. Leaver, F. Vazquez, S. W. Grill, and A. A. Hyman, Cell Rep **10**, 647 (2015).

[17] P. Askjaer, V. Galy, E. Hannak, and I. W. Mattaj, Mol. Biol. Cell **13**, 4355 (2002).

[18] Z. Bao and J. I. Murray, Cold Spring Harb Protoc **2011** (2011), ISSN 1559-6095 (Electronic) 1559-6095 (Linking).